J Mater Sci (2008) 43:5521–5526
DOI 10.1007/s10853-008-2785-9

Mg–6Zn/1.5%SiC nanocomposites fabricated by ultrasonic cavitation-based solidification processing

G. Cao · H. Choi · H. Konishi · S. Kou · R. Lakes · X. Li

Received: 13 December 2007 / Accepted: 6 June 2008 / Published online: 15 July 2008

Abstract Mg–6Zn/1.5%SiC nanocomposites were successfully fabricated by ultrasonic cavitation-based dispersion of SiC nanoparticles in Mg–6Zn alloy melt. As compared to un-reinforced Mg–6Zn alloy matrix, the mechanical properties of the nanocomposites including the tensile strength and yield strength of the Mg–6Zn/1.5%SiC nanocomposites were significantly higher; the good ductility of Mg–6Zn alloy matrix was retained. Nanoparticles were dispersed well though there were still some SiC microclusters in the microstructure. Also, the grain size of Mg–6Zn alloy was reduced considerably by the addition of 1.5%SiC nanoparticles.

Introduction

Metal matrix composites (MMCs) have emerged as an important class of materials capable of advanced structural, aerospace, automotive, electronic, thermal management, and wear applications [1]. Generally, about 15–60 vol.% microscale (10–50 μm) ceramic particulate or fiber reinforcements were added to the metal matrix. The major attractive features of MMCs are enhancement in stiffness, strength, creep resistance, fatigue resistance, and wear resistance [2]. But the ductility of MMCs is generally lower than the metal matrix [3]. The poor ductility of MMCs limits their widespread application areas where good ductility is required. Because the strength and modulus retention at high temperature of most ceramics are considerably greater than those of the metal matrix, the high-temperature performance is also improved significantly [4]. In fabricating the MMCs reinforced by powders/fibers/whiskers, some conventional methods such as stir casting, squeeze casting, and powder metallurgy were mostly used, some other processing techniques such as in situ synthesis, mechanical alloying, pressureless infiltration, gas injection, and spray forming were also sometimes used [3].

Because of the low density and superior specific strength of magnesium alloy, the usage of magnesium alloys in automotive industry has increased. The magnesium-based MMCs have also been extensively studied. Liang et al. [5] studied the AZ91 magnesium alloy reinforced by SiC particulates fabricated using the fluxless casting technique. The as-cast AZ91 reinforced by SiC particulates exhibited higher ultimate tensile and yield strengths at different temperatures, as well as the better wear-resistance at room temperature. Xi et al. [6] studied the SiC whiskers-reinforced MB15 magnesium matrix composites by powder metallurgy and found that the mechanical properties of SiC whiskers-reinforced MB15 composites were significantly influenced by powder-mixing methods of powder metallurgy. Li et al. [7] studied the hot deformation behavior of SiC whiskers-reinforced AZ91 composites in compression.

G. Cao · H. Choi · H. Konishi · X. Li (✉)
Department of Mechanical Engineering,
University of Wisconsin, Madison, WI 53706, USA
e-mail: xcli@engr.wisc.edu

G. Cao
e-mail: gcao@wisc.edu

S. Kou
Department of Materials Science and Engineering,
University of Wisconsin, Madison, WI 53706, USA

R. Lakes
Department of Engineering Physics, University of Wisconsin,
Madison, WI 53706, USA

The microstructure evolutions involved the movement of SiC whiskers and the changes of the matrix. The rotation and the fracture of SiC whiskers tended to be obvious with the increasing strain. High density of dislocations was observed in the AZ91 matrix at the initial stage of compression (1%). Jiang et al. [8] studied magnesium MMCs reinforced with B_4C particulates fabricated by powder metallurgy. The hardness and wear resistance of the composites were higher than those of the as-cast Mg ingot and increased with increasing amount of B_4C particulates from 10 to 20 vol.%. Zhang et al. [9] prepared carbon nanotube-reinforced magnesium MMC by stirring the carbon nanotubes into magnesium melts. It was found that carbon nanotubes, especially chemical nickel-plated ones, are excellent in magnesium strengthening. The structure of magnesium was refined. The tensile strength and elongation of the composite were also improved. Zheng et al. [10] studied the deformation and fracture behavior of as-solutionized SiC whiskers-reinforced AZ91 composites. The results indicated that the dislocation slip was impeded by the SiC whiskers and a large number of dislocation pile-ups occurred around the whiskers. Microcracks nucleated predominately at the SiC whisker-rich regions and the matrix near SiC–AZ91 interfaces. Pahutova et al. [11] studied the creep resistance of squeeze-cast AZ91 and QE22 magnesium alloys reinforced by 20 vol.% Al_2O_3 short fibers and showed that the creep resistance of reinforced materials was considerably improved compared to the monolithic alloys. Ye and Liu [3] reviewed the recent progress in magnesium matrix composites.

It was found at UW-Madison [12–16] that magnesium matrix nanocomposites (MMNCs) could be fabricated by adding a small percentage (less than 2 vol.%) of nano-size ceramic particles. The tensile properties including yield strength and ultimate tensile strength of MMNCs were improved significantly. The good ductility of magnesium alloy matrix was retained or even improved in MMNCs. As compared with conventional magnesium matrix composites reinforced by microparticles or fibers, the poor ductility of magnesium matrix composites was overcome. As predicted by an analytical model [17] of metal matrix nanocomposites, the mechanical properties of metals would be enhanced considerably if reinforced by ceramic nanoparticles (less than 100 nm). Moreover, similar to the magnesium matrix composites, MMNCs can also offer a significantly improved performance at elevated temperatures because thermally stable ceramic nanoparticles can maintain their properties at high temperatures.

To fabricate magnesium matrix composites reinforced by microparticles, solidification processing such as stir casting that utilizes mechanical stirring has been widely used. However, it is extremely challenging for the conventional mechanical stirring method to distribute and disperse nanoparticles uniformly in metal melts because of the much higher specific surface areas in nanoparticles. A new solidification processing technique, ultrasonic cavitation-based casting process, has been developed [18, 19]. It was found efficient in dispersing nanoparticles in metal melts. It was reported [20] that ultrasonic cavitation could produce transient (in the order of nanoseconds) micro "hot spots" that could have temperatures of about 5000 °C, pressures above 1000 atm, and heating and cooling rates above 10^{10} K/s. The strong impact coupled with local high temperatures can break nanoparticle clusters and clean the particle surface. Since nanoparticle clusters are loosely packed together, air, inert gas, or metal vapor can be trapped inside the voids in the clusters to serve as nuclei for ultrasonic cavitations.

By utilizing the ultrasonic cavitation-based solidification processing method, some magnesium alloys and A356 aluminum alloy enhanced by SiC nanoparticles have been fabricated successfully [12–16, 18, 19]. In this article, the microstructure and overall mechanical properties of Mg–6Zn/1.5%SiC nanocomposites (Mg–6Zn with 1.5 wt.% SiC nanoparticles) fabricated by ultrasonic cavitation-based solidification processing will be studied.

Experimental

Figure 1 shows the schematic experimental setup for the ultrasonic cavitation-based fabrication of nano-sized SiC-reinforced MMNCs. It mainly consisted of a resistance heating furnace for melting magnesium alloys, a nanoparticle-feeding mechanism, a gas protection system, and an ultrasonic processing system. A mild steel crucible with a capacity of about 1.5 kg (about 3.0 lbs) was used for melting and ultrasonic processing. The ultrasonic processing system was made by Advanced Sonics, LLC, Oxford, CT. An ultrasonic probe made of C103 niobium alloy was used for ultrasonic processing. The ultrasonic probe was activated by a transducer fabricated from the Permendur magnetostrictive alloy. The Permendur alloy offered the ability to convert high-power electrical energy into mechanical motion. The transducer was activated with a fluctuating magnetic field. As the strength of the magnetic field increased, the length of the Permendur alloy also increased.

About 800 g of pure (99.8%) magnesium was first melted in a mild steel crucible. When the temperature of the melt reached 700 °C, pure (99.99%) Zn (up to 6 wt.%) was added into the pure magnesium melt. The melt was stirred manually for 3 min to make homogenous Mg–6Zn melt. Then the ultrasonic probe, which is 35 mm in diameter and 292 mm in length, was dipped into the melt and the melt was processed ultrasonically at a power level of 3.5 kW. The processing frequency was 17.5 kHz. The

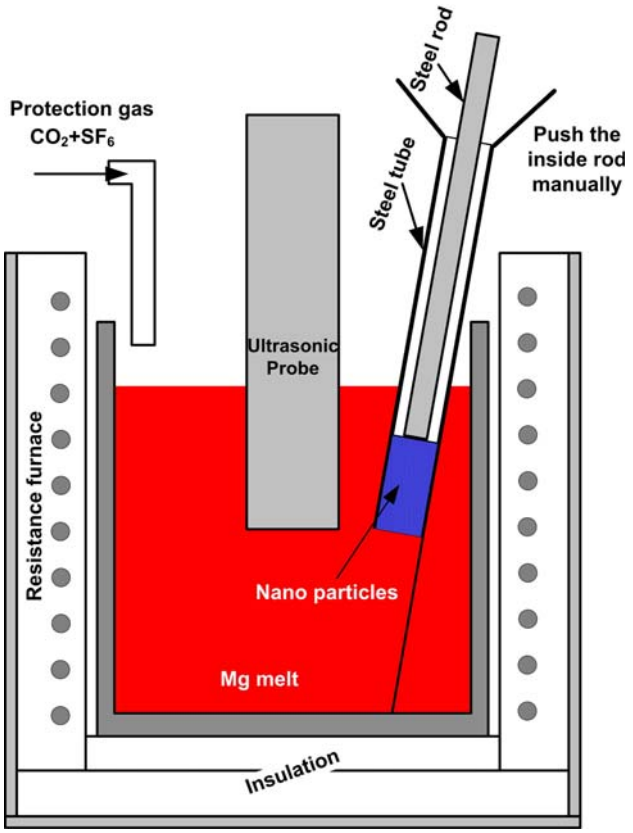

Fig. 1 Experimental setup for fabricating Mg–6Zn/1.5%SiC nanocomposites

peak-to-peak displacement of the ultrasonic probe was about 40 μm. During ultrasonic processing, about 1.5 wt.% SiC nanoparticles were slowly fed into the Mg melt through a steel tube by pushing down the inside steel rod in the tube. Each time only about 0.5 g SiC nanopowders could be pushed into the Mg alloy melt. It took about 45 min to feed 1.5 wt.% powders. The SiC nanopowders were supplied by Nanostructured and Amorphous Materials Inc, Houston, Texas. The average size of the SiC particles was 50 nm. The ultrasonic probe was dipped 32 mm into the melt. The melt was protected by CO_2 + 0.75% SF_6 gas flowing through three steel tubes positioned near the melt surface. A K-type thermocouple with a steel protection tube was put in the melt to control the temperature of the melt. The melt temperature for ultrasonic processing was controlled at about 700 °C. After all the powder was fed into the magnesium melt, the steel feed tube was removed and the ultrasonic processing continued for another 15 min. After ultrasonic processing, the ultrasonic probe was lifted and the temperature of the magnesium alloy melt was increased to the pouring temperature in about 5–10 min. Then the whole steel crucible was lifted to cast the magnesium melt into a steel permanent mold preheated to 400 °C with a resistance heater. The pouring temperature was 735 °C. In each casting, two standard tensile specimens were made, each with a gage length of 44.5 mm and a diameter of 9.5 mm. An additional graphite pouring cup was used to guide the melt and served as the housing for a SiC ceramic foam filter. The filter, 55 mm × 55 mm × 12 mm in dimension and about 1.25 mm in pore diameter, effectively filtered away magnesium oxide films. Some of the castings for tensile testing were T5 heat treated. T5 stands for heat treatment at 330 °C for 2 h followed by air cooling, and then at 180 °C for 16 h followed by air cooling.

The tensile properties of the Mg–6Zn/1.5%SiC nanocomposites specimens were tested with a Sintech 10/GL machine. The tensile testing was conducted in accordance with ASTM B 557M-07. Before the tensile testing, both ends of the 44.5 mm gage length of the specimens were marked and the original gage length was measured. An extensometer with a 1" (25.4 mm) gage length was clamped to each tensile sample. The cross head speed was 5 mm/min. When the strain reached 1%, the tensile testing machine paused temporally for the extensometer to be removed. At the first stage of tensile testing, the strain data came from the extensometer. After the extensometer was removed, the tensile testing continued until the sample failed. The yield strength and ultimate tensile strength were determined from the stress and strain data recorded in the computer. After tensile testing, the two fractured ends were fitted together with matched surfaces and the final gage length was measured. The elongation of the sample was calculated based on the measurements of the original and final gage lengths.

The microstructure of the samples was studied by optical microscopy and scanning electron microscopy (SEM). The specimens for optical microscopy and SEM were prepared first by grinding with 240, 400, 800, and 1200 grit SiC abrasive papers and then by mechanical polishing with 1 μm and 0.1 μm diamond slurries. SEM was conducted on a LEO 1530 machine. Specimens for transmission electron microscopy (TEM) were prepared by ion milling. Specimens for ion milling were prepared by polishing until they were approximately 30–50 μm thick. The polished samples were mounted on a Mo TEM grid and then ion milled. A low-angle ion beam (less than 10°) was used to avoid preferential etching. TEM measurements was done on a Philips CM 200UT microscope equipped with a NORAN Voyager energy dispersive X-ray spectrometry system, operating at 200 kV (point-to-point resolution 0.19 nm and spherical aberration coefficient $C_s = 0.5$ mm).

Results and discussion

Figure 2a and b shows the average results of tensile testing at the room temperature. As shown in Fig. 2a, the yield

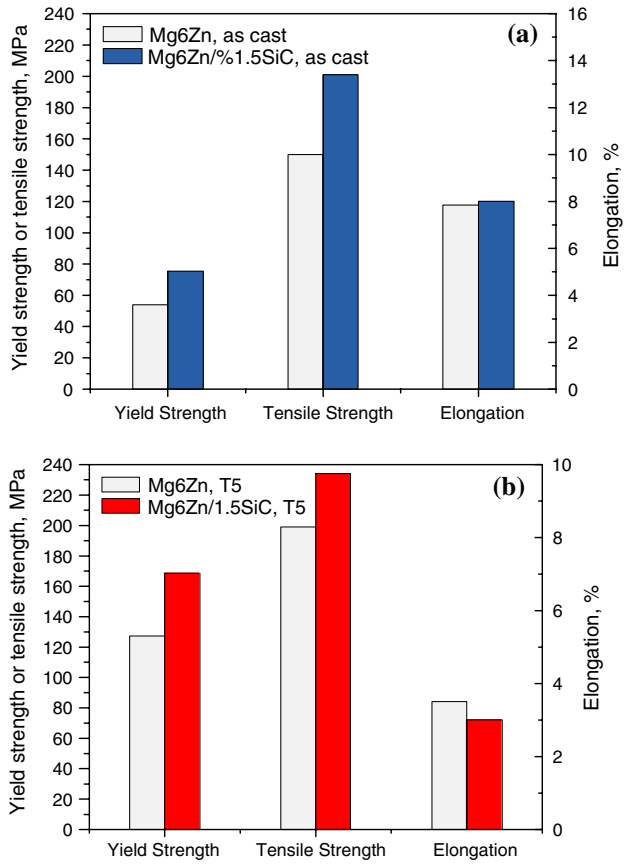

Fig. 2 Mechanical properties of Mg–6Zn and Mg–6Zn/1.5%SiC in the (**a**) as-cast and (**b**) after T5 heat treatment

strength and ultimate tensile strength of Mg–6Zn in the as-cast condition were 54 and 150 MPa, respectively. For Mg–6Zn/1.5%SiC nanocomposites, the yield strength and ultimate tensile strength are increased to 76 and 201 MPa, respectively. The yield strength is increased by 40% and the ultimate tensile strength by 34%. The elongation of Mg–6Zn alloy in the as-cast form is 7.7%. The elongation of Mg–6Zn/1.5%SiC nanocomposites is similar to that of Mg–6Zn. This good ductility of MMNCs contrasts with the magnesium matrix composites reinforced by microparticles or microfibers, in which the ductility is normally reduced considerably. Poor ductility in MMCs is a problem for a lot of applications in various industries. After the T5 heat treatment, both Mg–6Zn and Mg–6Zn/1.5%SiC nanocomposites become significantly stronger, as shown in Fig. 2b. The yield strength and tensile strength of Mg–6Zn/1.5%SiC are still significantly higher than those of Mg–6Zn while the ductility is about the same. This good combination of strength and ductility can position MMNCs as a promising class of structural materials for future automotive and aerospace applications. The tensile testing shows that dispersed SiC nanoparticles are efficient in strengthening the Mg–6Zn alloy. According to a recently

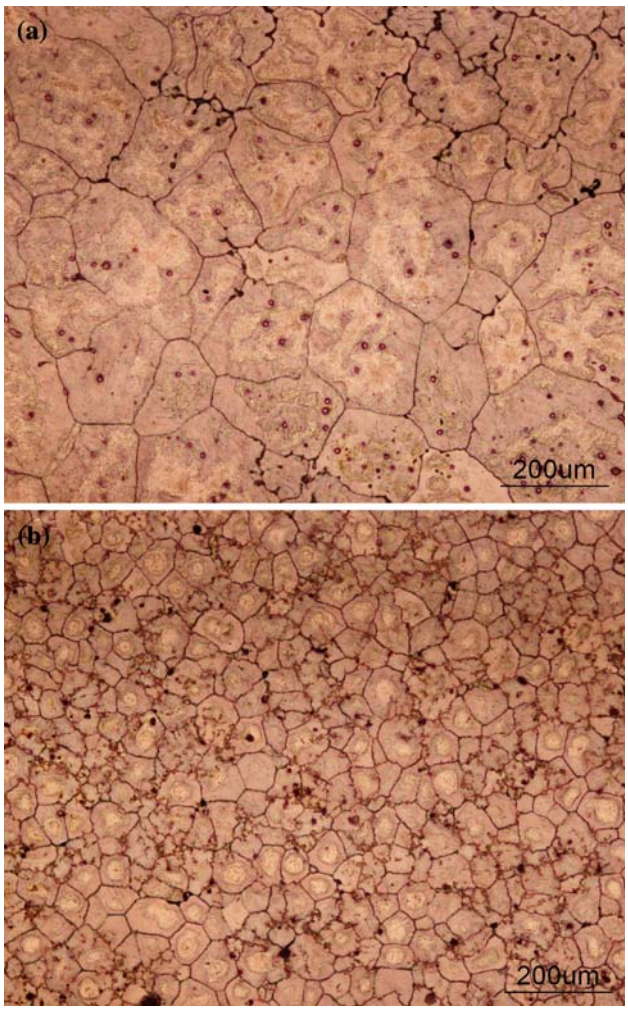

Fig. 3 Optical image of (**a**) Mg–6Zn matrix and (**b**) Mg–6Zn/1.5%SiC nanocomposites. The grain size in Mg–6Zn/1.5%SiC is refined significantly

published analytical model [17] for predicting the yield strength of metal matrix nanocomposites, the strengthening induced by nanoparticles can be attributed to the Orowan strengthening effect, enhanced dislocation density, and load-bearing effects. It should be pointed out that Orowan strengthening is not significant in traditional MMCs. However, it becomes more favorable in metal matrix nanocomposites because the Orowan bowing phenomenon allows dislocations to bypass the dispersed nanoparticles. A small volume fraction of nanoparticles is adequate to significantly improve the yield strength of metal matrix nanocomposites without compromising ductility.

Figure 3 shows the optical microstructure of the Mg–6Zn alloy and Mg–6Zn/1.5%SiC nanocomposite. The samples were taken from the crosssection at the end of the gage section in the tensile samples, thus representing the true microstructure of the tensile bars. It should be noted that the grain size of Mg–6Zn was reduced significantly by the addition of SiC nanoparticles in the Mg–6Zn/1.5%SiC

nanocomposite. According to the classic Hall–Petch equation: $\sigma_y = \sigma_0 + K_y d^{-1/2}$, where σ_y is the yield strength, σ_0 and K_y are material constants, and d is the mean grain size. The value of K_y is dependent on the number of slip systems. It is higher for HCP metals than for FCC and BCC metals [3]. Since Mg is HCP, the grain size affects the yield strength significantly. It is also well known that the grain size has a strong effect on the ductility and toughness of materials. During solidification processing of Mg–6Zn/1.5%SiC, SiC nanoparticles served as nuclei for heterogeneous nucleation and refined the grains. The no loss of ductility could be, in part, attributed to the significantly refined grain size in Mg–6Zn/1.5%SiC. Moreover, the castability of Mg–6Zn was also improved by the addition of 1.5%SiC nanoparticles. The castability of Mg–6Zn was not good because the solidification range of Mg–6Zn is rather wide as compared to other magnesium alloys such as Mg–Al alloys. A more detailed study on castability enhancement by the addition of a small amount of SiC nanoparticles in Mg–Zn alloys is underway.

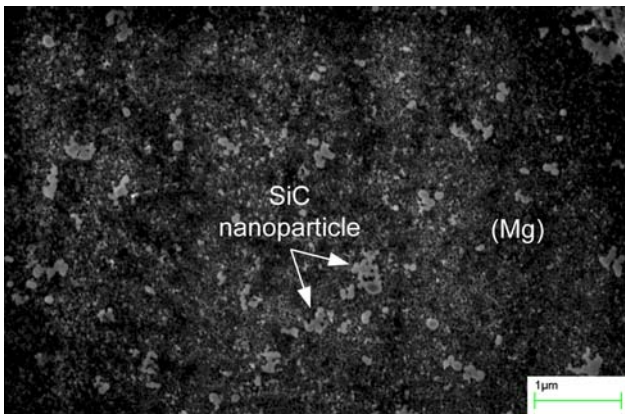

Fig. 4 SEM image of dispersed SiC particles in Mg–6Zn/1.5%SiC

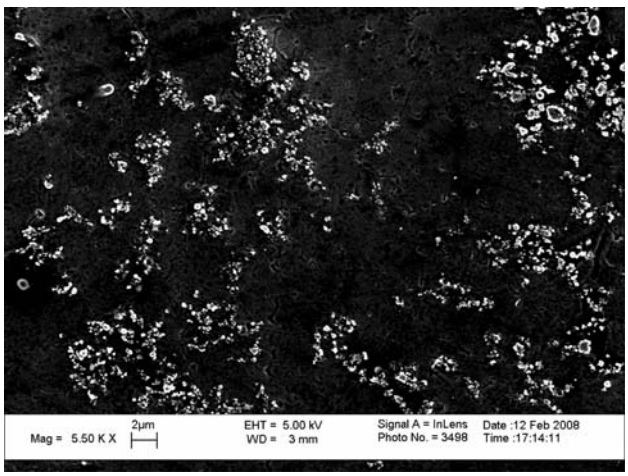

Fig. 5 SEM image of SiC clusters in Mg–6Zn/1.5%SiC; the white spots are SiC particle clusters and the dark background is Mg matrix

As shown by the SEM image of Mg–6Zn/1.5%SiC in Fig. 4, some dispersed nanoparticles can be seen clearly. This level of dispersion is very difficult to reach via mechanical stirring. But it should be pointed out that some nanoparticles are still agglomerated or maybe even sintered in the Mg–6Zn/1.5%SiC, as shown in Fig. 5. Actually, from the low-magnification optical image (Fig. 3b) of the Mg–6Zn/1.5%SiC, some larger SiC microclusters can also be seen. Figures 3b and 5 show that the SiC nanoparticles were not dispersed completely. Further improvement in the extent of nanoparticle dispersion is desired. Since there are quite a few microclusters of SiC, one could expect the ductility of Mg–6Zn/1.5%SiC nanocomposites to be reduced by the clusters. However, the tensile testing showed that the ductility of Mg–6Zn/1.5%SiC nanocomposites was actually similar to that of Mg–6Zn matrix. This can be explained from the following two aspects. Firstly, inside the small clusters, SiC microclusters were still separated mostly by magnesium between the nanoparticles. These SiC clusters could be deformed more easily during tensile testing than the microscale SiC particles in magnesium matrix composites. Secondly, the negative effects of SiC microclusters were balanced by the positive effects of grain refining. In the case of Mg–6Zn/1.5%SiC, if all the

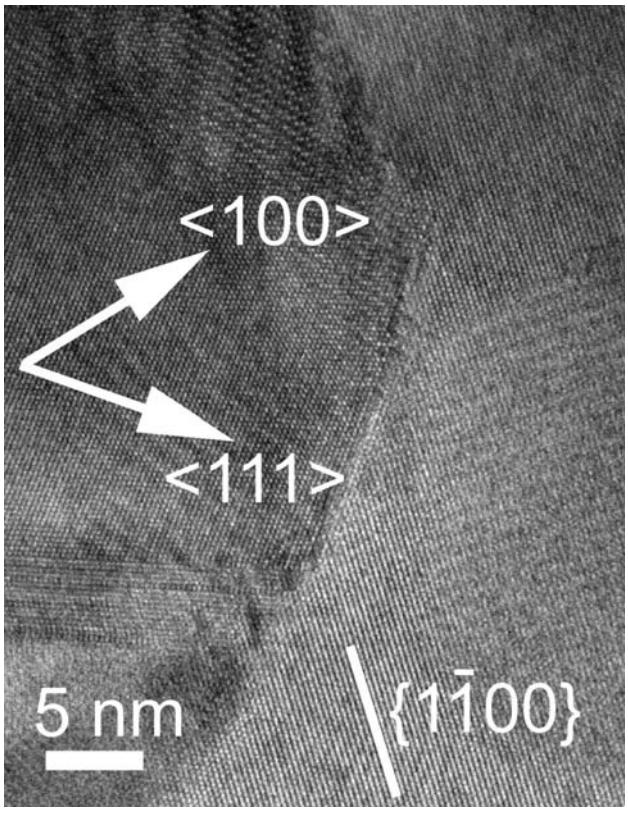

Fig. 6 HRTEM image of the interface between SiC particle and Mg alloy matrix. The left side is SiC and the right side is the Mg alloy matrix

microclusters can be dispersed into separated independent nanoparticles, the mechanical properties can be improved even more.

Figure 6 shows a high-resolution transmission electron microscopy (HRTEM) image of the interface between a SiC particle and the magnesium alloy matrix. No intermediate phase was observed at the interface. This indicated that the SiC nanoparticles bonded well with the Mg alloy matrix.

Conclusion

Ultrasonic cavitation-based solidification processing allows nanoparticles to be incorporated in an alloy matrix. The resulting nanocomposite is stronger than the monolithic alloy. Ultrasonic cavitation is effective in dispersing nanoparticles in molten Mg–6Zn to prepare for MMNCs. While some microclusters of SiC still existed in the matrix, the grain size of Mg–6Zn alloy was reduced significantly by the addition of SiC nanoparticles. The ultimate tensile strength and yield strength were increased significantly. The good ductility of Mg–6Zn matrix was retained in Mg–6Zn/1.5%SiC nanocomposite. TEM image of the interface between the SiC nanoparticles and Mg–6Zn alloy matrix showed that SiC nanoparticles had bonded well with the Mg–6Zn alloy matrix.

Acknowledgement This work was supported by National Science Foundation 0506767.

References

1. Koczak MJ, Khatri SC, Allison JE, Bader MG (1993) In: Suresh S, Mortensen A, Needleman A (eds) Fundamental of metal-matrix composites. Butterworth-Heinemann, New York, p 297
2. Clyne TW, Withers PJ (1993) An introduction to metal matrix composites. Cambridge University Press, Cambridge, pp 454–457
3. Ye HZ, Liu XY (2004) J Mater Sci 39:6153
4. Wawner FE (1994) In: Noor AK, Venneri SL (eds) Advanced metallics, metal-matrix and polymer-matrix composites—assessment and future directions, vol 2. The American Society of Mechanical Engineers, New York, pp 162–163
5. Liang L-C, Bai Y, Yang Y-S, Wang Y, Chen L-J (2007) Shenyang Gongye Daxue Xuebao (J Shenyang Univ Technol) 29:139
6. Xi YL, Chai DL, Zhang WX, Zhou JE (2005) Rare Met Mater Eng 34:1131
7. Li SB, Gan W, Zheng M, Wu K (2005) Trans Nonferr Met Soc China 15:245
8. Jiang QC, Wang HY, Ma BX, Wang Y, Zhao F (2005) J Alloy Compd 386:177
9. Zhang Y, Xue Y, Li S, Huang J, Huang C (2005) Mater Sci Forum 488–489:897
10. Zheng MY, Zhang WC, Wu K, Yao CK (2003) J Mater Sci 38:2647
11. Pahutova M, Sklenicka V, Kucharova K, Svoboda M (2003) Int J Mater Prod Technol 18:116
12. Li X, Duan Z, Cao G, Roure A (2007) Trans Am Found Soc 115:747
13. Cao G, Konishi H, Li X (2008) Mater Sci Eng A 486(1–2):357
14. Cao G, Kobliska J, Konishi H, Li X (2008) Metall Mater Trans A 39(4):880
15. Cao G, Konishi H, Li X (2008) J Manuf Sci Eng 130:031105-1
16. Cao G, Konishi H, Li X (2008) Int J Metalcast 2:57
17. Zhang Z, Chen DL (2006) Scr Mater 54:1321
18. Lan J, Yang Y, Li X (2004) Mater Sci Eng A 386:284
19. Yang Y, Li X (2007) ASME J Manuf Sci Eng 129:252
20. Suslick KS, Didenko Y, Fang MM, Hyeon T, Kolbeck KJ, McNamara WB, Mdleleni MM, Wong M (1999) Philos Trans R Soc A 357:335